

## ELECTRO-ACOUSTIC RESPONSE AT THE FOCAL POINT OF A FOCUSED TRANSDUCER AS A FUNCTION OF THE ACOUSTICAL PROPERTIES OF THE LENS

**P. Marechal, F. Levassort, L.-P. Tran-Huu-Hue and M. Lethiecq**

Laboratoire d'UltraSons Signaux et Instrumentation-GIP ULTRASONS,

Université François Rabelais, Tours, France

[marechal@univ-tours.fr](mailto:marechal@univ-tours.fr)

### Abstract

Focusing ultrasound is needed for high resolution imaging applications such as non destructive testing (NDT) or medical imaging. Its effects are explored in the case of a single-element transducer focused with a lens, and electrically driven with a broad-band excitation. The electro-acoustic response very near the surface of the transducer is first modelled using a finite element method (ATILA). This response in the very near-field is then propagated in water thanks to two codes. These results are presented and compared. Using these tools, the electro-acoustic response is investigated at the focal point, as a function of the acoustical impedance of the lens.

### Introduction

The use of focused ultrasound is necessary for many applications such as NDT and medical imaging. In order to obtain a good trade-off in terms of lateral resolution and depth of field, the f-number which is the ratio between the focal distance  $F$  and the diameter of the transducer is often between 2 and 3. Moreover, according to typical lens material properties, the focal distance is between 3 and 6 times the radius of curvature. These two conditions impose a range of values for the radius of curvature of the lens which is between one and two radius of the piezoelectric disk (highly focused configuration). Consequently, a 2D axisymmetric resolution scheme can be used. We chose to take advantage of the finite element method (FEM), with the ATILA software, which can take into account both longitudinal and radial components.

The aim of this study is to determine the influence of a focusing lens (and corresponding acoustical properties) on the pressure field at the focal point.

Many investigations dealing with the radiation of a focused transducer have shown that there is no analytical solution even for classical harmonic excitation [1], so that some approximations have to be made.

Here, FEM is used to calculate the electro-acoustic response to a broad-band excitation very near the surface of the focused transducer. Two propagation codes, a method based on the Discrete Hankel Transform (DHT) [2] and the numerical integration method of the Rayleigh integral (NIM) [3, 4] are then used to compute the electro-acoustic response

up to the focal point. Finally, a performance index defined for imaging applications is presented as a function of the acoustical impedance of the lens, while the focusing distance is kept constant.

### Configuration and material properties

For this study, the configuration retained is a high frequency single element transducer based on a piezoelectric disk bounded on the rear face by a backing and on the front face by a matching layer and a lens (Figure 1). The piezoelectric material is a lead titanate ceramic (Ferroperm Pz 34) with a thickness of 50  $\mu\text{m}$  corresponding to a centre frequency of the simulated transducer at 43 MHz.

To determine the other material properties (acoustical impedance and thickness) of the backing and matching layer, an optimisation method is used. This method calculates the electro-acoustic response of the transducer with an equivalent electrical scheme (KLM unidimensional model) to deduce a value of a performance index defined as:

$$x = 30 \log(d_{20}) + 20 \log(d_{40}) - 10 \log(\text{amp}) \quad (1)$$

where  $d_{20}$  and  $d_{40}$  are respectively the time durations at  $-20$  and  $-40$  dB of the gaussian envelope, and  $\text{amp}$  is the amplitude of the envelope of the electro-acoustic response. This index allows to obtain an appropriate electro-acoustic response in term of trade-off between sensitivity and axial resolution, specifically for imaging applications [5].

The minimisation of this index by a recursive algorithm delivers, with the corresponding electro-acoustic response, the optimal properties of the backing and matching layer (Table 1).

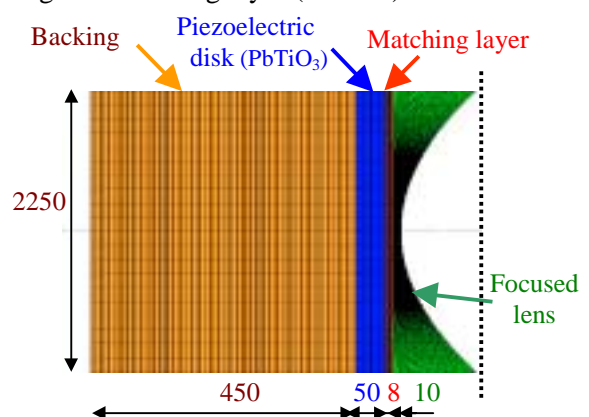


Figure 1: Mesh and dimensions ( $\mu\text{m}$ ) of the single element transducer.

Table 1 : Properties of the different elements ( $Z$  is the acoustical impedance,  $\rho$  the density,  $c_L$  and  $c_S$  are the longitudinal and shear wave velocities,  $l_L$  is the length along the  $z$  propagation axis normalised by the wavelength, and  $n_L$  the mesh density given in mesh per wavelength).

	Backing	Piezoelectric disk	Matching layer	Focusing lens	Water
$Z$ (MRa)	3.8	35	6.8	2.2	1.5
$\rho$ (kg/m <sup>3</sup> )	1815	7550	3930	1035	1000
$c_L$ (m/s)	2120	4630	1725	2100	1490
$c_S$ (m/s)	1005	2675	850	1060	-
$l_L$ ( $\lambda$ )	9	1/2	1/4	1/4	-
$n_L$ (mesh/ $\lambda$ )	5	16	16	9	8

The diameter of the transducer has also been chosen (Figure 1), according to the dielectric constant of the piezoelectric element, to have an electrical impedance at the centre frequency near 50  $\Omega$ .

The optimised mesh for FEM calculation is chosen in term of trade-off between precision and calculation time in order to fit the first harmonic of the impulse response at the transducer's surface (along the dotted line in Figure 1). In the same way the radial mesh is determined to allow edge wave propagation in water. The mesh density is given in Table 1 as a function of the wavelength.

The acoustical impedance of the lens is chosen to vary from that of water (i.e. 1.5 MRa) up to 5 MRa in order to determine the which gives optimal properties of the electro-acoustic response of the transducer.

From the acoustical impedances deduced (backing, matching layer) or chosen (lens), an homogenisation model is used (ATA model) to calculate the corresponding wave velocities ( $c_L$  and  $c_S$ ) in epoxy resin loaded with metallic particles. These results, used as inputs for the ATILA software, are given in Table 1 and Figure 2 for the lens.

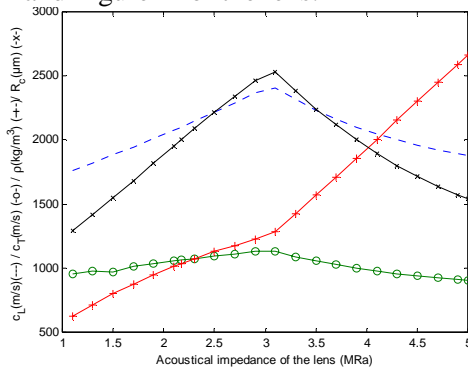


Figure 2 : Properties of the lens (- -  $c_L$  (m/s), -o-  $c_S$  (m/s), -+-  $\rho$  (kg/m<sup>3</sup>), -x-  $R_c$  ( $\mu$ m)) as a function of its acoustical impedance.

The focal distance in the case of a strongly focused lens is derived from the ray theory and is given by:

$$F = \frac{a^2}{2 \left( 1 - \frac{c_0}{c_L} \right) \left( R_c - \sqrt{R_c^2 - a^2} \right)} \quad (2)$$

where  $a$  is the radius of the transducer,  $R_c$  is the lens radius of curvature,  $c_0$  and  $c_L$  are the longitudinal wave velocities in the propagation medium and in the lens (Figure 3). The radius of curvature  $R_c$  is then chosen to keep constant the focal distance  $F$  (6.3 mm) in all simulations given by (2) (see Figure 2 for the variation of  $R_c$  as a function of  $Z_{lens}$ ).

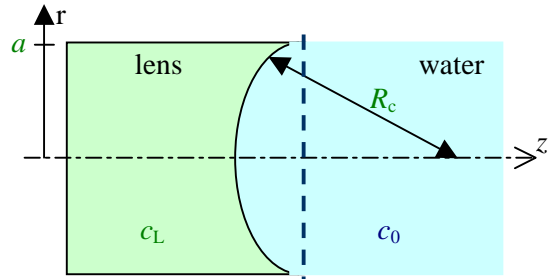


Figure 3: Geometry and parameters of the lens.

### Propagation models

Once the electro-acoustic response is known in a plane in water (as shown in dashed line on Figure 1), the pressure field is computed using two propagation codes which are briefly described.

#### Discrete Hankel Transform

The Hankel transform or the Fourier Bessel transform is a simplified formulation of a bidimensional Fourier transform in the case of axisymmetric geometry. It is used in the frequency domain, i.e. in the  $(k, \omega)$  space.

The pressure field  $p(r, z, t)$  is known in a plane, extracted as a result of a radially symmetric FEM calculation. A Fourier transform then permits a plane wave decomposition, from  $p(r, z, t)$  to  $p(r, z, \omega)$ .

Similarly to the bidimensional Fourier transform for a bidimensional geometry,

$$P(k_x, k_y, z, \omega) = \int_{-\infty}^{+\infty} \int_{-\infty}^{+\infty} p(x, y, z, \omega) \cdot e^{-j(k_x x + k_y y)} dx dy \quad (3)$$

the Hankel transform expresses the axisymmetric expression  $p(r, z, \omega)$  in the  $(k_r, z, \omega)$  space:

$$P(k_r, z, \omega) = \int_0^{+\infty} p(r, z, \omega) J_0(k_r r) r dr \quad (4)$$

A discrete Hankel transform [2, 6] was implemented. Once the pressure is expressed in the  $(k, \omega)$  space, the analytical  $z$ -delay function is used as a propagation operator, either in its radial space form, called the spatially sampled convolution (SSC) or in its radial frequency form, called the frequency sampled convolution (FSC). This last solution is a very fast way to calculate the pressure field on a whole radial plane for each calculation step.

A major improvement of the FSC, called ray theory-updated frequency sampled convolution (RFSC), consists in a decrease of the propagation wave-number to its significant values [2].

### Numerical Integration Method

The numerical integration method is based on the Rayleigh integral:

$$p(x, y, z, t) = j\omega\rho \iint_S \frac{e^{j(\omega t - kR)}}{2\pi R} v dS \quad (5)$$

where  $R$  is the distance between the point source and the observation point,  $S$  the surface, and  $v$  the point source velocity. It is then decomposed in a sum of contributions of small size elements (as compared to the near-field distance), so that the far-field approximation is verified [3, 4].

$$p(x, y, z, t) = j\omega\rho \sum_{m,n} \frac{e^{j(\omega t - kR_{m,n})}}{2\pi R_{m,n}} v_{m,n} \Delta x_m \Delta y_n \quad (6)$$

Each active sub-element of step  $a_n$  is calculated in order to satisfy the far field assumption, with:

$$n_{nearfield} = \frac{z}{L_{nearfield}} = \frac{z}{a_n^2 / \lambda} = 400 \quad (7)$$

so the size of a sub-element is given by:

$$a_n = \sqrt{\frac{\lambda z}{n_{nearfield}}} \quad (8)$$

These calculation methods were implemented and validated with harmonic excitations on a piston transducer for which the analytical solution is known. Moreover, the results obtained in the case of a focused transducer were compared to the classical approximated solution [1], and a good agreement was found.

## Results

### Propagation code comparison

The on-axis pressure (Figure 4) is nearly the same for the NIM, DHT-SSC, DHT-RFSC methods, from the most accurate (NIM) to the faster (DHT-RFSC). For a high resolution calculation, the NIM is the most accurate, but the calculation can be time consuming. The main advantage of the DHT methods is that they give directly the pressure in a whole radial plane, so the lateral resolution is known at each calculation step.

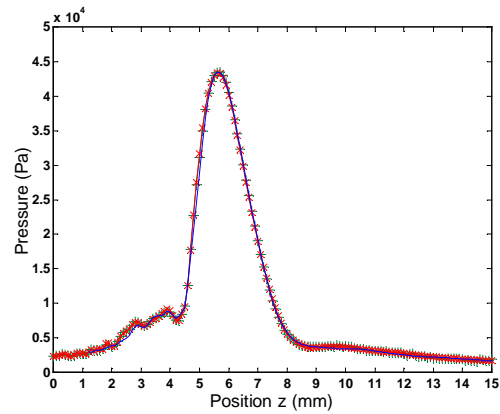


Figure 4 : On-axis pressure (--- NIM, +- DHT-SSC, -x- DHT-RFSC).

A good accuracy is obtained with the DHT-SSC and a low precision but faster calculation with the DHT-RFSC.

At the focal point, we have computed and characterised the electro-acoustic response (Figure 5) for a given configuration of the transducer. The NIM and DHT-SSC are in good agreement up to  $-60$  dB, and can therefore be used. But, the DHT-RFSC algorithm is less adapted than the two other since errors appear at  $-40$  dB. Finally, for a chosen on-axis  $z$  position, the calculation time difference is negligible, and the accuracy is comparable for the NIM and DHT-SSC.

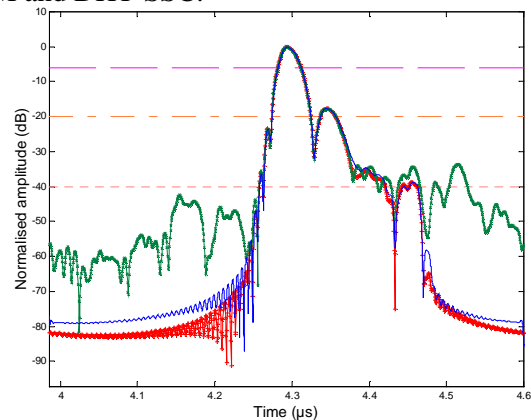


Figure 5 : Normalised envelope of the impulse response at the focal point (--- NIM, +- DHT-SSC, -x- DHT-RFSC).

### Influence of a focusing lens

The calculation of the electro-acoustic response at the focal point has been performed (ATILA+NIM) for several values of lens acoustical impedance. The performance index (1) has been calculated for each configuration.

The results with a lens are first compared to those obtained by replacing the focusing lens by a second matching layer, using the one dimensional KLM model.

The obtained KLM optimal values range from 1.7 to 2.5 MRa, while those of propagated FEM results (Figure 6) vary between 3.3 to 4.1 MRa.

This can be explained by the fact that neither the propagation nor the focusing are taken into account with the KLM simulation.

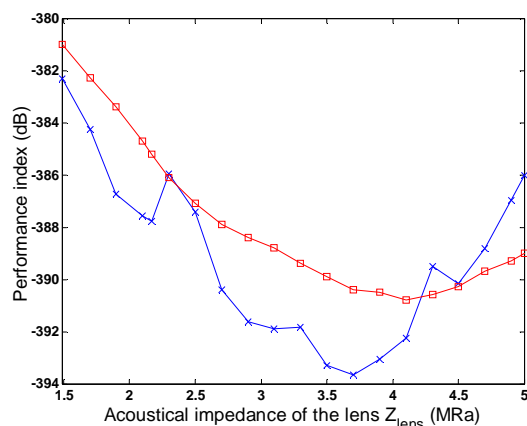


Figure 6 :Imaging performance index  $x$  (-□- KLM and propagation filtering, -x- ATILA and NIM propagation).

Consequently, the KLM result at the transducer's surface needs to be propagated, taking into account the acoustical focusing generated by the lens. This calculation (Fig. 6, -□-) is performed thanks to a propagation filter using the NIM propagation code described earlier.

The performance index curve is smoother for the KLM propagated result (Figure 6, -□-) than for the ATILA propagated result (Figure 6, -x-). This can be explained by the fact that with KLM, there is no disruption from radial modes, whereas it is the case in the ATILA simulations.

The performance index curves are slightly different, but the optimal range of values are very similar.

The optimal range of values for the acoustical impedance of the lens is nearly the same with 3.5 to 4.7 MRa and 3.3 to 4.1 MRa respectively for propagated KLM and ATILA results.

Dispersion of the acoustic energy can also be observed on the impulse response at the focusing point (Figure 7).

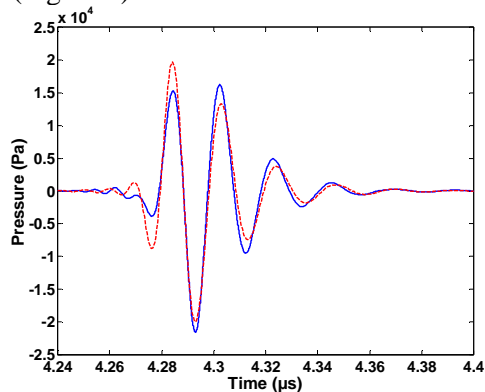


Figure 7 : Impulse response at the focal point for  $Z_{lens} = 4.1$  MRa (KLM and propagation filtering, ATILA and NIM propagation).

Nevertheless, the pulses are very similar, and even if the beginning is slightly different, the measured characteristics are the same: the amplitude and the duration at -20 and -40 dB are equal within a few percent.

### Conclusion and perspectives

An optimisation of properties for imaging applications was performed on a single element transducer, as a function of the acoustical impedance of the focusing lens. The focal spot was calculated using a modelling of the longitudinal and radial modes with the finite element method, using ATILA software and a propagation code. The characterisation of the focal spot, in sensitivity and axial resolution, was investigated through a performance index.

The optimal range of values obtained with the propagated KLM results is nearly the same as that of propagated ATILA results. Thus the propagated KLM result, considering only longitudinal modes, is an interesting fast alternative way to determine the optimal range of acoustical impedance of the lens.

For a global optimisation of the transducer, the electrical excitation waveform must be investigated in order to obtain an impulse response corresponding to imaging application requirements.

### References

- [1] B.G. Lucas and T.G. Muir, "The field of a focusing source", *J.A.S.A.*, Vol. 72, N°4, pp. 1289-1296, 1982.
- [2] P.T. Christopher and K.J. Parker, "New approaches to the linear propagation of acoustic fields", *J.A.S.A.*, Vol. 90, N°1, pp. 507-521, 1991.
- [3] K.B. Ocheltree and L.A. Frizzell, "Sound field calculation for rectangular sources", *IEEE Trans on Ultrason., Ferro. and Freq. Cont.*, Vol. 36, N°2, pp. 242-248, 1989.
- [4] C. Lee and P.J. Benkeser, "Computationally efficient sound field calculations for a circular array transducer", *IEEE Trans on Ultrason., Ferro. and Freq. Cont.*, Vol. 39, N°1, pp. 43-47, 1994.
- [5] L.P. Tran-Huu-Hue, R. Desmare, F. Levassort and M. Lethiecq, "A K.L.M. circuit-based method for modeling multilayer piezoelectric structures", *IEEE Ultrasonics Symposium*, pp. 995-998, 1997.
- [6] H.F. Johnson, "An improved method for computing a discrete Hankel transform", *Computer and Physics Comm.*, Vol. 43, pp. 183-202, 1987.

### Acknowledgement

This work was funded by the E.U. in the on-going GROWTH FP5 project PIRAMID.